Applied Surface Science 277 (2013) 167–175

Contents lists available at SciVerse ScienceDirect

Applied Surface Science

journal homepage: www.elsevier.com/locate/apsusc

# Effect of an *in situ* hydrogen plasma pre-treatment on the reduction of GaSb native oxides prior to atomic layer deposition

Erin R. Cleveland*, Laura B. Ruppalt, Brian R. Bennett, S.M. Prokes

*Electronics Science and Technology Division, U.S. Naval Research Laboratory, Washington, DC, United States*

ARTICLE INFO

*Article history:*
Received 2 February 2013
Received in revised form 29 March 2013
Accepted 2 April 2013
Available online 12 April 2013

*Keywords:*
GaSb
Hydrogen plasma
Atomic layer deposition
TMA
XPS
III–V semiconductors

ABSTRACT

The influence of an *in situ* hydrogen plasma pre-treatment on the modification of native oxides of GaSb surfaces prior to atomic layer deposition (ALD) is presented. The effects of varying rf-plasma power, exposure time, and substrate temperature have been characterized by atomic force microscopy (AFM), *ex situ* X-ray photoelectron spectroscopy (XPS), as well as capacitance–voltage (*C–V*) measurements on fabricated devices. Results indicate that a completely oxide free surface may not be necessary to produce a good electrical interface with a subsequent ALD $Al_2O_3$ dielectric; the most effective hydrogen plasma treatments resulted in the absence of Sb-oxides, a reduction in elemental Sb, and an increase in the $Ga_2O_3$ content at the interface. The use of an *in situ* hydrogen plasma pre-treatment eliminates the need for wet chemical etches and may also be relevant to the deposition of other high-*k* dielectrics, making it a promising technique for realizing high performance Sb-based MOS-devices.

© 2013 Elsevier B.V. All rights reserved.

## 1. Introduction

III–V compound semiconductors are attracting widespread attention as an alternative material to Si in advanced complementary metal–oxide–semiconductor (CMOS) applications; their high electron and hole mobilities, as well as relatively narrow bandgaps make them increasingly attractive for high-speed, low power applications [1–4]. A significant amount of work already exists on n-channel III–V metal–oxide–semiconductor field-effect transistors (MOSFETs) demonstrating excellent electron mobility and high drive currents [4–7]. However, hole mobility in III–V p-channel MOSFETs typically lags in comparison to Si [6]. Among the III–V semiconductors, GaSb is a promising material for both n- and p-channel devices due to its high electron and hole mobilities (bulk mobility ~6000 $cm^2/Vs$ and 850 $cm^2/Vs$, respectively), which are found to be amongst the highest of the III–V semiconductor materials [6]. However, the poor quality of the gate oxide/GaSb interface has limited the use of GaSb in microelectronics. Unlike the silicon-silicon dioxide interface pair, the native oxide found on GaSb is complex in structure and composition, forming heavily defected interfaces that pin the semiconductor Fermi-level near midgap and limit the device's ability to modulate charge.

The increasing need to integrate high-*k* dielectric thin films into CMOS structures has led researchers to turn to atomic layer deposition (ALD) for insulator growth. ALD is a gas phase deposition technique that utilizes self-limiting chemistries in order to produce thin solid films with excellent atomic-level thickness control [8]. ALD is widely accepted as a means to produce high quality films over large surface areas with excellent uniformity and conformality [8,9]. These key attributes are inherent to the self-limiting nature of the ALD surface reactions: alternating reactant exposures of two gaseous precursors create a saturated chemisorbed surface which leads to film growth one sub-monolayer at a time [8]. The sequential behavior of the precursor exposures helps avoid the formation of gas-phase particles and creates thin, continuous, pin-hole-free films that are critical to the operation of CMOS devices. Therefore, particular attention should be focused on the development of techniques to form low-defect interfaces between III–V surfaces and high-*k* films deposited by ALD.

GaSb is known to have a highly reactive surface [10–12]. On exposure to air it will form a complex native oxide composed of not only Sb-oxides and Ga-oxides, but elemental Sb as well [12,13]. Therefore, a significant effort has been focused on surface preparations prior to ALD that remove native oxides and passivate GaSb atoms in order to ensure the best possible interface [14]. Current approaches for oxide removal primarily consist of wet etches, such as HCl [6,7,10,12,15], HF [15], $(NH_4)_2S$ [13,16], and $NH_4OH$ [15,16]; however, due to the rapid re-oxidation of the GaSb after oxide removal and a general lack of reproducibility, a better means of interface cleaning is desirable. Recent progress in the field of ALD on III–Vs has led researchers to a proposed "self-cleaning" mechanism through the use of the ALD precursor trimethylaluminum

* Corresponding author. Tel.: +1 2024041165.
*E-mail address:* erin.cleveland.ctr@nrl.navy.mil (E.R. Cleveland).

0169-4332/$ – see front matter © 2013 Elsevier B.V. All rights reserved.
http://dx.doi.org/10.1016/j.apsusc.2013.04.018

(TMA), in which the native oxides are consumed during the initial TMA half-cycle [6,12,16–19]. While effective, this process has not been proven to be standalone for oxide removal, as it is typically preceded by a wet chemical etch that removes the bulk of the native oxide. Alternatively, hydrogen ($H_2$) plasma cleaning has been considered a potential candidate for efficient low temperature oxide removal from III–V semiconductors during molecular beam epitaxy (MBE) regrowth processes [20–23]. Under appropriate conditions, it has been shown that $H_2$-plasma treatments in ultra-high vacuum can result in high quality, defect-, impurity-, and oxide-free GaSb surfaces [19,20]. These observations suggest the usefulness of a $H_2$ plasma process for surface preparation prior to ALD, as well; however, to fully utilize this potential requires a full understanding of the oxide removal process and its effect on surface composition and roughness of the remaining surface.

In this work, we first evaluate the effectiveness of TMA as a standalone process by investigating the removal of native oxides on GaSb surfaces that have undergone no additional wet chemical treatment. Subsequently, we examine the use of an *in situ* $H_2$ plasma pre-treatment as a means to obtain a suitable electrical interface prior to the deposition of high-*k* $Al_2O_3$ films on GaSb substrates *via* plasma-enhanced ALD (PEALD). *Ex situ* X-ray photoelectron spectroscopy (XPS) and atomic force microscopy (AFM), as well as capacitance–voltage (*C–V*) measurements, were performed to establish the effect of the rf-plasma power, substrate temperature, and plasma exposure time on the growth interface. Results indicate that a completely oxide-free surface may not be necessary to produce a good electrical interface.

## 2. Experimental

Epitaxial layers of GaSb (*p*-type, Be-doped $2 \times 10^{17}$ cm$^{-3}$) were grown *via* molecular beam epitaxy (MBE) on bulk GaSb (100) wafers (unintentionally doped p-type). The substrate temperature was 460 °C, and the growth rate was 0.5 monolayers/s. Growth interrupts were used to ensure a smooth surface. The recipe was 55 repeats of 60 s GaSb/20 s $Sb_2$ interrupt, yielding 500 nm of GaSb.

Samples were allowed to oxidize in air at room temperature for one day and then cleaved into 3 mm × 5 mm pieces. Samples were loaded into a Beneq TFS-200 ALD viscous flow-type reactor equipped with a UHV load-lock chamber and setup in a remote plasma configuration. Plasmas were generated by capacitive coupling using a 13.56 MHz rf-power source. The distance between the sample and the grid, which acts as the bottom electrode, was 4 cm and ensured that samples were not in direct contact with the plasma. The $H_2$ plasma pre-treatment was typically performed using a rf plasma power of 50 W at a substrate temperature of 150 °C for 10 min, with the exception of when a plasma parameter was being investigated. Hydrogen gas (99.999%) was mixed with argon (99.999%) to ensure plasma ignition. The hydrogen and argon gases had flow rates of 20 sccm and 140 sccm, respectively. During plasma processing, the pressure within the reaction chamber was 1.5 Torr. After plasma exposure, samples were coated with 6 μ-pulses of the ALD precursor, trimethylaluminum (TMA). All TMA exposures were done at 150 °C and each μ-pulse was 150 ms followed by a 1 s argon purge to remove potentially reactive species from the reaction chamber.

Samples were unloaded from the ALD reactor and analyzed using an *ex situ* monochromatic X-ray photospectroscopy (XPS) with an Al Kα source in order to assess the subsequent surface chemistry. XPS spectra were fit with Thermo Avantage software using a Shirely baseline and corrections were made for charge shifting when the C 1s peak was not found to be at 285 eV. Investigations of the resulting surface morphology were performed using an *ex situ* Digital Instruments Atomic Force Microscope (AFM) (MultiMode™ NanoScope® IV) in tapping mode with Si tips. AFM scans were taken over areas of 1 μm × 1 μm, 4 μm × 4 μm, and 10 μm × 10 μm.

To assess the electrical quality of the oxide/semiconductor interface, p-type GaSb (1 0 0) MOS capacitors were fabricated with high-*k* $Al_2O_3$ deposited *via* PEALD from TMA and oxygen plasma. $Al_2O_3$ films were deposited at a substrate temperature of 150 °C on $H_2$ plasma treated GaSb epilayer surfaces for 100 cycles, resulting in film thicknesses of ~16 nm. Film thicknesses were verified using *in situ* ellipsometry on concurrent silicon wafers. After the dielectric deposition, samples were annealed in a forming gas mixture of 9:1 $N_2/H_2$ at 350 °C for 30 min. MOS capacitors were fabricated and consisted of a Ti/Au (100/1000 Å) e-beam evaporated top gate, an oxide mesa defined using aqueous 10:1 buffered oxide etch, and a Pd/Pt/Au (120/100/1000 Å) e-beam evaporated top-side ohmic substrate contact. Frequency-resolved capacitance–voltage (*C–V*) measurements were acquired using a semiconductor characterization system at room temperature.

## 3. Results

### 3.1. TMA vs $H_2$ plasma

TMA half-cycle exposure has often been cited as a means for "self-cleaning" III–V surfaces prior to $Al_2O_3$ ALD [16,18]. However, its effectiveness as a standalone process, without prior use of wet chemical etches, has yet to be demonstrated. Furthermore, since all samples in this study were exposed to a TMA-passivation following the $H_2$ plasma treatment, it is important to understand the role of the TMA precursor in the oxide removal. Therefore, we compared the use of TMA without a wet chemical treatment, a $H_2$ plasma without TMA, and the combination of a $H_2$ plasma followed by exposure to TMA.

Fig. 1 displays XPS Sb 3d and Ga 3d core level spectra associated with the as-grown GaSb epilayer covered with a native oxide layer consisting of Sb-oxides and Ga-oxides as indicated by a shift to higher binding energies with respect to the "bulk" substrate features at 528 eV for Sb $3d_{5/2}$ and 19.1 eV for Ga 3d [11,16]. Detailed non-linear curve fitting for both the Sb 3d and the Ga 3d core levels (Fig. 1) indicates that Sb-oxide appears in the +4 ($Sb_2O_4$) valence form, which is a mixture of both $Sb_2O_5$ and $Sb_2O_3$ [11], and Ga-oxide is comprised of both the +1 state ($Ga_2O$) and the +3 state ($Ga_2O_3$), with peak positions found at 530.5 eV ($Sb_2O_4$), 20.1 eV ($Ga_2O$), and 20.7 eV ($Ga_2O_3$) [11,18]. The AFM image of Fig. 3a demonstrates the amorphous quality of the native oxide of the untreated GaSb surface, with an RMS roughness of 0.67 nm.

TMA-only samples were exposed to 6 μ-pulses of the TMA precursor (less than 1 s total exposure time) in order to ensure complete surface saturation. XPS spectra from this sample are plotted in Fig. 2b, with the as-grown epilayer data repeated in Fig. 2a for comparison. As evident by both the Sb 3d and the Ga 3d spectra, a considerable amount of oxide is left on the surface after TMA exposure. While oxide clearly remains, it is believed that overall, the native oxide was reduced by the TMA as indicated by the observation of an Al—O peak in the Al 2*p* spectra (not shown here), as well as the appearance of atomic terraces seen in the AFM image of Fig. 3b. The underlying principle of ALD is that it is a self-limiting process: once the surface is saturated with TMA, no more precursor can be adsorbed. Since there was no oxidizer half-cycle, the oxygen in the Al—O bonds had to come from a ligand exchange between the GaSb native oxide and the TMA precursor. Once the initial layer of $Al_2O_3$ was formed, no further reduction of the native oxide could take place by additional exposure to TMA, limiting the "clean up" effect of the TMA to only the first few monolayers. This is especially critical in the GaSb system, since the native oxide is on the order of 3–5 nm [10,11] thick, which is considerably greater than that found on Si.

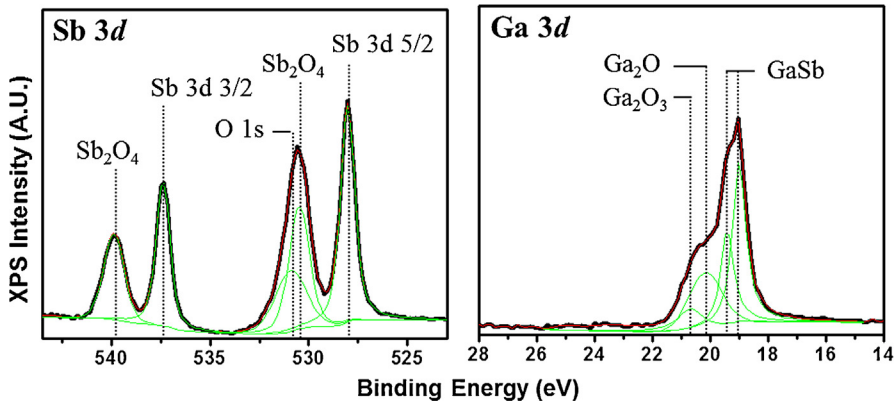


**Fig. 1.** Detailed non-linear curve fitting of both the Sb 3d and the Ga 3d XPS core level spectra of the untreated as-grown GaSb epilayer.

In contrast to the TMA treatment, samples exposed to a 50 W, 150 °C $H_2$ plasma pre-treatment for 10 min (Fig. 2c) exhibit complete removal of $Sb_2O_4$ with an unexpected increase in $Ga_2O_3$. Note that the peak found at binding energy 531.5 eV in the Sb 3d spectra is due solely to the O 1s and not an oxide shifted Sb $3d_{5/3}$ core level [16]. For this peak to be associated with Sb-oxide there would have to be a companion Sb $3d_{3/2}$ feature as seen in the untreated and TMA exposed samples. Furthermore, subsequent TMA exposures following a $H_2$ plasma pre-treatment (Fig. 2d) do not appear to have any added influence in the removal of Ga-oxides. However, the slight decrease in the Sb 3d core level and Ga 3d GaSb peak intensities can be attributed to thicker $Ga_2O_3$ and $AlO_x$ over-layers. While TMA treatments may be effective at removing several monolayers of native oxide, as evident by the presence of atomic terraces in Fig. 3b, exposure to a $H_2$ plasma prior to TMA is effective at both structurally and chemically transforming the native oxide layer, as evident by XPS.

Although TMA has been shown to be limited in the removal of native oxides from the GaSb surface, it has proven to be a good passivant. Hydrogen plasma treated samples, free of Sb-oxides, were coated with 6 μ-pulses of TMA to ensure complete surface saturation. After storage in a nitrogen dry box environment for approximately five months, samples were re-characterized *via* XPS. XPS measurements indicated that the surface remained Sb-oxide free and the amount of $Ga_2O_3$ had not increased.

### 3.2. *Effect of $H_2$ plasma power*

Epitaxially grown GaSb (1 0 0) samples were exposed to a $H_2$ plasma pre-treatment with plasma powers varying from 25 W to 100 W for 10 min at a substrate temperature of 150 °C. Following plasma exposure, samples were passivated with 6 μ-pulses of TMA prior to removal from vacuum. The effect on the surface morphology as a function of the $H_2$ plasma power was measured by AFM, as shown in Fig. 3. In contrast to the relatively rough, amorphous native oxide found on the untreated GaSb surface (Fig. 3a), samples exposed to $H_2$ plasma (Fig. 3c–f), reveal single atomic steps on the order of 0.3 nm corresponding to approximately 1 monolayer. An increase in plasma power leads to an increase in the kinetic energy and possibly the density of plasma species. As a consequence there

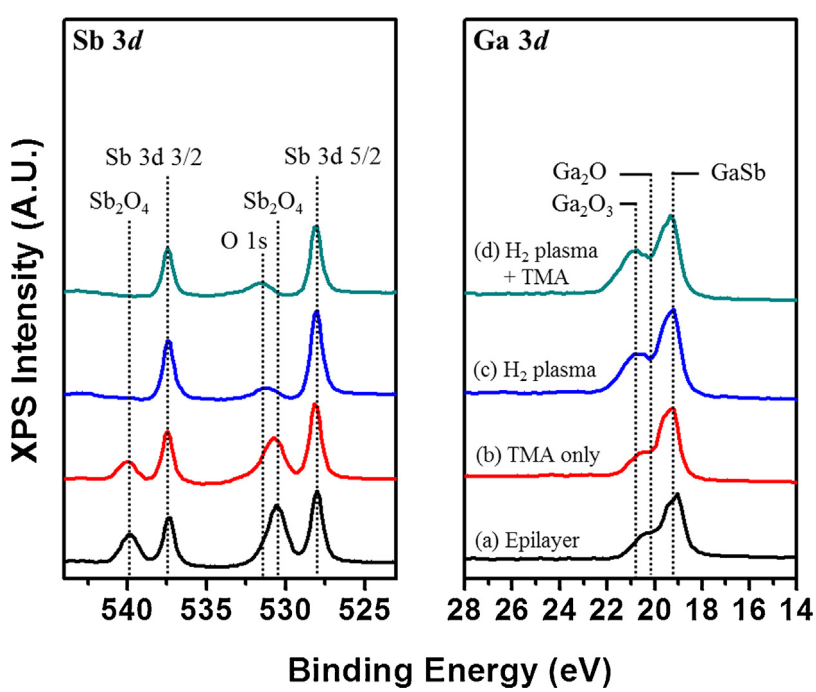


**Fig. 2.** Sb 3d and Ga 3d core-level XPS spectra for (a) the untreated 500 nm thick GaSb epilayer with native oxide, after exposure to (b) only TMA, (c) only an $H_2$ plasma, and (d) an $H_2$ plasma followed by TMA.

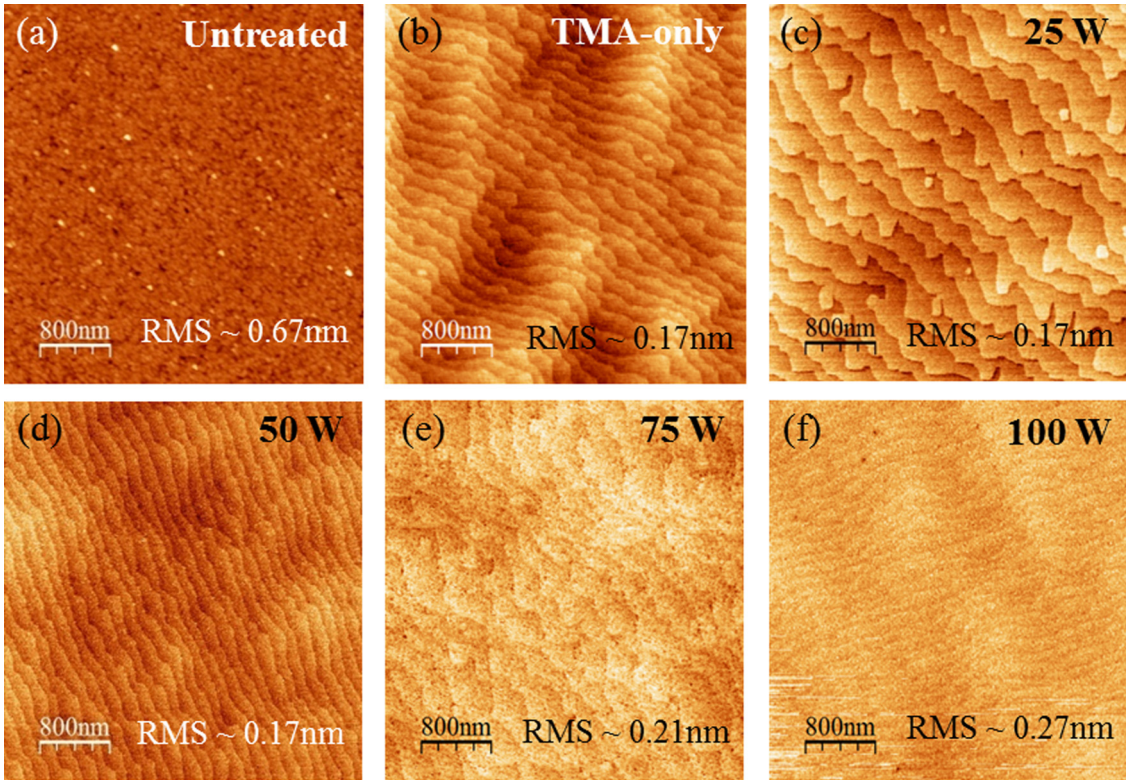


**Fig. 3.** 4 μm × 4 μm AFM images of an (a) untreated 500 nm thick GaSb epilayer surface with native oxide, (b) after exposure to only TMA, and after exposure to a $H_2$ plasma for 10 min with varying plasma powers of (c) 25 W, (d) 50 W, (e) 75 W, and (f) 100 W. Plasma exposure was followed by a TMA exposure for samples (c)–(f). (Atomic steps within images (b)–(f) are aligned with respect to sample orientation.)

is an increase in surface etching with increased plasma power; generally producing shorter terrace widths, smoother leading edges, and decreasing the peak-to-valley height. Overall, the surfaces appear more uniform as plasma power increases.

Fig. 4 plots the high-resolution XPS spectra of the Sb 3d and Ga 3d core levels for (a) the untreated native-oxide covered GaSb epilayer and samples exposed to a $H_2$ plasma with a power of (b) 25 W, (c) 50 W, (d) 75 W, and (e) 100 W. The Sb 3d spectra of the untreated epilayer (Fig. 4a) shows both spin-orbit components, Sb $3d_{5/2}$ and Sb $3d_{3/2}$, with additional peaks positioned at higher binding energies relative to the substrate peaks, indicative of the Sb—O chemical shift. Detailed non-linear curve fitting of both the Sb 3d and the Ga 3d for the untreated GaSb epilayer indicate a native oxide present on the surface composed of $Sb_2O_4$, $Ga_2O$, and

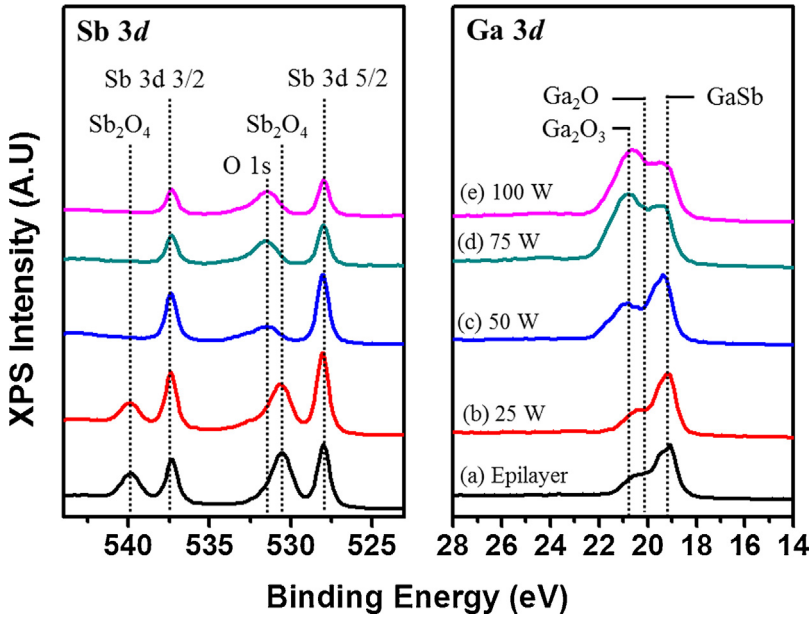


**Fig. 4.** Sb 3d and Ga 3d core-level XPS spectra for (a) the untreated 500 nm thick GaSb epilayer with native oxide and after exposure to an $H_2$ plasma for 10 min with varying plasma powers of (b) 25 W, (c) 50 W, (d) 75 W, and (e) 100 W. Following plasma exposure, samples (b)–(e) were coated with TMA.

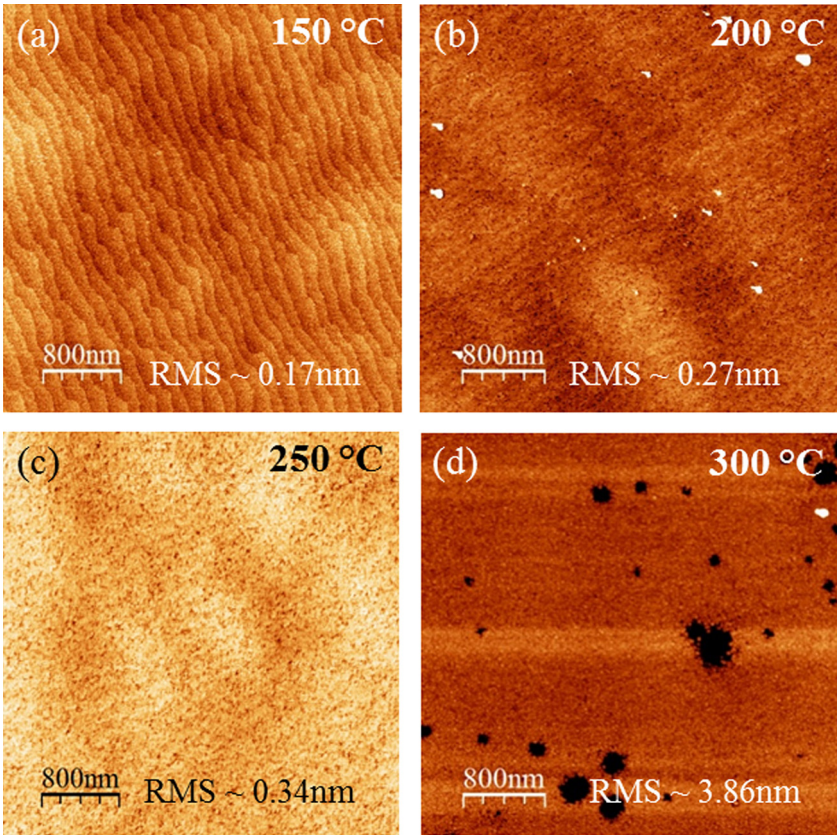


**Fig. 5.** 4 μm × 4 μm AFM images of a 500 nm thick GaSb epilayer surface after exposure to a 50 W $H_2$ plasma for 10 min at various substrate temperatures: (a) 150 °C, (b) 200 °C, (c) 250 °C, and (d) 300 °C. Plasma exposure was followed by a TMA exposure for all samples. (Atomic steps within images (a)–(c) are aligned with respect to sample orientation.)

$Ga_2O_3$. Samples exposed to a 25 W plasma show very little change in either the Sb—O or Ga—O peaks; however, as the plasma power was increased, the $Sb_2O_4$ was completely removed. Additionally, a reduction in the Sb $3d_{5/2}$ and Sb $3d_{3/2}$ peak intensities is observed for plasma powers greater than 50 W (Fig. 4c–e). This decrease in intensities is attributed to a decrease in elemental Sb and not attenuation due to a $Ga_2O_3$ over-layer, since the intensity of the GaSb peak seen in the Ga 3d spectra remains constant. Although a plasma power of 50 W or greater is adequate in removing Sb-oxides from the surface, that does not appear to be the case for the Ga-oxides. The increase in intensity at higher binding energies indicates a redistribution of oxygen from the Sb to the Ga, creating a more $Ga_2O_3$ rich surface, as shown in Fig. 4c–e.

### 3.3. Effect of substrate temperature during $H_2$ plasma exposure

Experiments were carried out to examine the influence of substrate temperature on the reduction of native oxides found on the GaSb surface during exposure to a $H_2$ plasma. Epitaxially grown GaSb (1 0 0) samples were exposed to a $H_2$ plasma pre-treatment for 10 min with a plasma power of 50 W for the substrate temperatures 150 °C, 200 °C, 250 °C, and 300 °C. Fig. 5 demonstrates the effect of the substrate temperature on the surface morphology as measured by AFM. Scans for substrate temperatures of 150–250 °C (Fig. 5a–c) reveal single atomic terraces on the order of 0.3 nm in step height. As the substrate temperature increases, terrace widths become shorter, the peak-to-valley height decreases, and an increase in the RMS roughness is observed. In addition, Fig. 5d reveals a very rough surface with a significant amount of pitting when the substrate temperature was raised to 300 °C. This behavior is due to Sb out diffusing through the substrate and eventually desorbing from the surface; leaving a Ga-rich surface, where the Ga migrates and creates droplets across the surface, as seen in 1 μm × 1 μm AFM scans (not shown here).

Fig. 6 displays XPS spectra of the GaSb sample with (a) the initial native oxide and those exposed to a 50 W $H_2$ plasma for 10 min for four different temperatures: (b) 150 °C, (c) 200 °C, (d) 250 °C, and (e) 300 °C. The Sb 3d spectra indicate that the $Sb_2O_4$ is completely removed for all substrate temperatures, as noted by the lack of a companion peak on the Sb $3d_{3/2}$. Furthermore, a reduction in elemental Sb is observed for increased substrate temperatures, with 250 °C (Fig. 6d) exhibiting the weakest Sb 3d peak intensity. In association with increased substrate temperature, an increase in the $Ga_2O_3$ peak intensity is observed indicating a transfer of oxygen from Sb to Ga, as well as the development of a $Ga_2O_3$ over-layer. The mild increase in surface roughness seen in Fig. 5a–c is attributed to the elemental Sb desorption. Conversely, when the substrate temperature was raised to 300 °C (Fig. 6e), there was a resurgence of the Sb 3d peak intensities, as well as a decrease in the $Ga_2O_3$. The Ga—Ga bonding expected from the presence of the Ga droplets is obscured by the GaSb peak in the Ga 3d spectra.

### 3.4. Effect of $H_2$ plasma exposure time

MBE grown GaSb (1 0 0) samples were exposed to a 50 W $H_2$ plasma pre-treatment for 1, 5, 10, 20, 30, and 60 min exposure times at a substrate temperature of 150 °C. The influence of the plasma exposure time on the surface morphology as measured by AFM is seen in Fig. 7. Upon plasma exposure, atomic terraces with steps on the order of 0.3 nm are revealed. However, prolonged exposure led to an increase in surface etching, where by 60 min (Fig. 7f) the

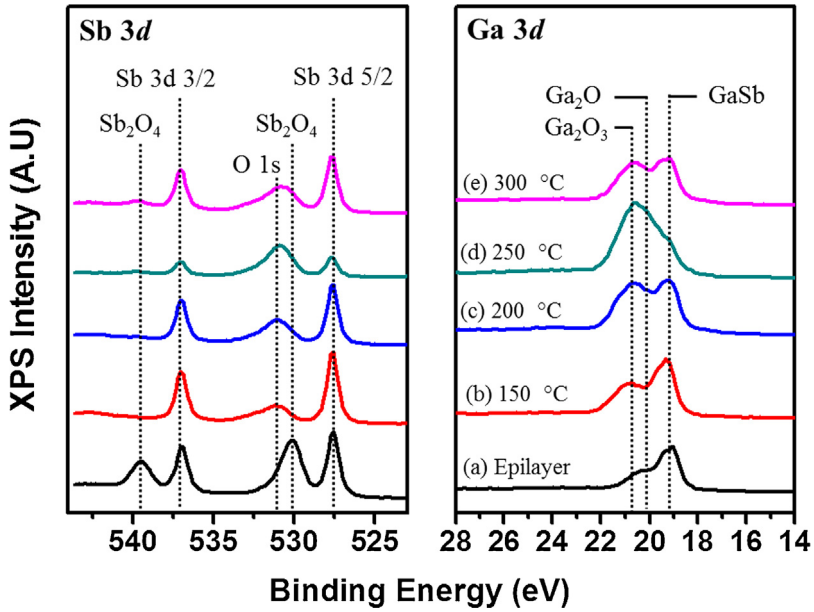


**Fig. 6.** Sb 3d and Ga 3d core-level XPS spectra for the (a) untreated 500 nm thick GaSb epilayer with native oxide and after exposure to a 50 W $H_2$ plasma for 10 min at various substrate temperatures: (b) 150 °C, (c) 200 °C, (d) 250 °C, and (e) 300 °C. Following plasma exposures samples were coated with TMA.

atomic terraces are almost gone; yet, the RMS roughness did not greatly increase after a 1 min exposure (Fig. 7b).

Fig. 8 shows the evolution of the Sb 3d and Ga 3d core levels as a function of the plasma exposure time. Samples exposed to a $H_2$ plasma for 10 min or longer (Fig. 8b–e) exhibit complete removal of the $Sb_2O_4$. Furthermore, very little change in the Sb $3d_{5/2}$ and Sb $3d_{3/2}$ peak intensities is seen, suggesting there was little to no additional removal of elemental Sb. Additionally, the increase in the O 1s peak intensity for the 20 min exposure corresponds to the increase in $Ga_2O_3$, as seen in the Ga 3d core spectra. Longer exposure times had little added influence on the surface composition after 20 min.

### 3.5. Electrical characterization

To assess the electrical quality of the oxide/semiconductor interface, *C–V* measurements were made on circular MOS capacitors ranging from 60 μm to 100 μm in diameter [1]. Fig. 9 plots the *C–V* characteristics for frequencies ranging from 4 kHz to 2 MHz for capacitors on p-type GaSb with four different $H_2$ plasma pretreatments: (a) the untreated GaSb epilayer, (b) a 100 W plasma power for 10 min at a substrate temperature of 150 °C, (c) 50 W plasma power for 10 min at a substrate temperature of 250 °C, and (d) a 50 W plasma power for 20 min at a substrate temperature of 150 °C. The untreated sample (Fig. 9a) shows a virtually static

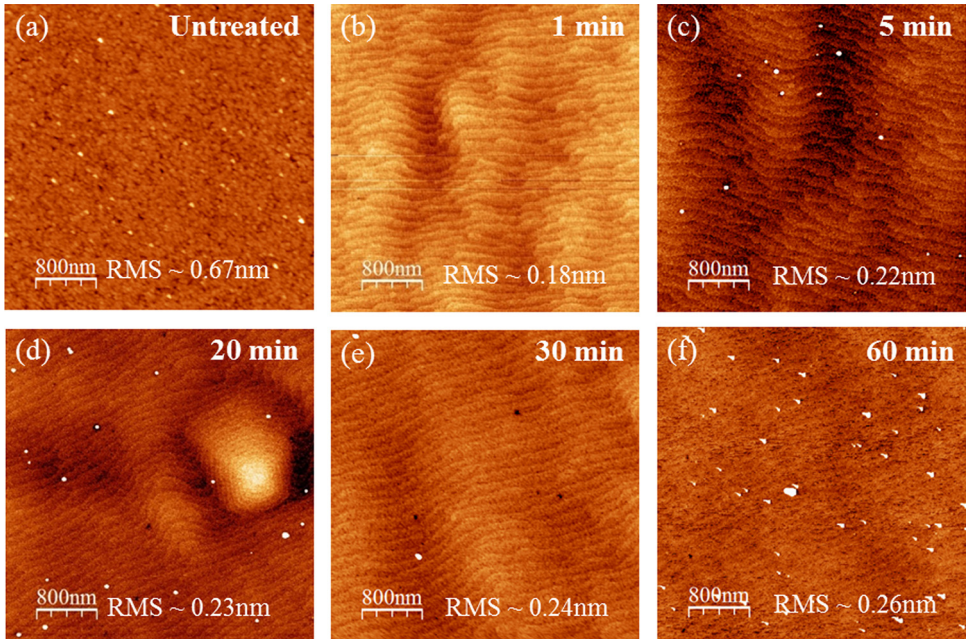


**Fig. 7.** 4 μm × 4 μm AFM images of a (a) 500 nm thick GaSb epilayer surface with native oxide and after exposure to a 50 W $H_2$ plasma for: (b) 1 min, (c) 5 min, (d) 20 min, (e) 30 min, and (f) 60 min. Plasma exposure was followed by a TMA exposure for samples (b)–(f). (Atomic steps within images (b)–(f) are aligned with respect to sample orientation.)

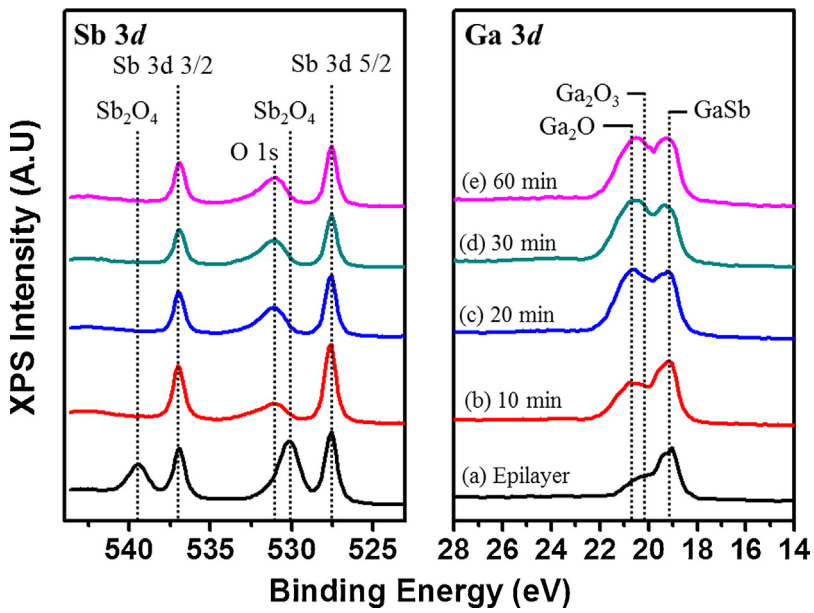


**Fig. 8.** Sb 3d and Ga 3d core-level XPS spectra for the untreated 500 nm thick GaSb epilayer (a) and after exposure to a 50 W $H_2$ plasma at a substrate temperature of 150 °C for (b) 10, (c) 20, (d) 30, and (e) 60 min. Following plasma exposures samples were coated with TMA.

capacitance regardless of applied gate bias, indicating a pinned Fermi-level at the insulator/semiconductor interface and suggesting a high density of interface states that prevents adequate Fermi-level movement within the semiconductor. Additionally, a significant amount of frequency dispersion is seen in accumulation over the given frequency range, a further indication of interface or near-interface trap states. However, *C–V* measurements of samples exposed to a $H_2$ plasma (Fig. 9b–d) display the familiar frequency variation expected for MOS capacitors, indicating that the Fermi-level is sufficiently unpinned to sweep the semiconductor from accumulation through depletion to inversion. Additionally, the amount of frequency dispersion in accumulation decreased,

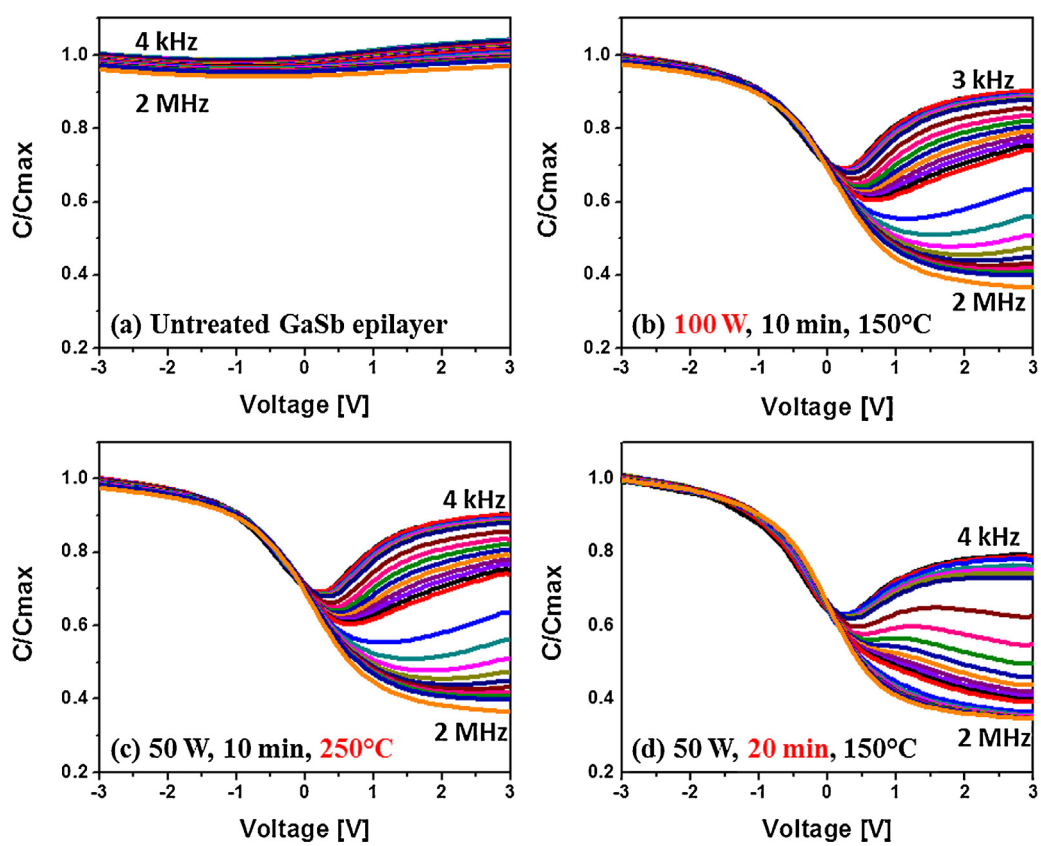


**Fig. 9.** Frequency-resolved *C–V* measurements for GaSb MOS capacitors fabricated on (a) an untreated GaSb substrate and on substrates exposed to $H_2$ plasma pretreatments using best case plasma parameters: (b) 100 W, 10 min, 150 °C, (c) 50 W, 10 min, 250 °C, and (d) 50 W, 20 min, 150 °C.

representing a reduction in trap states near the valence band. Not all treated samples showed unpinned *C–V* performance; however, good capacitance characteristics were achieved by independently increasing the plasma power (≥100 W), plasma exposure time (≥20 min), and the substrate temperature (up to 250 °C). Samples exhibiting the highest capacitance modulation (Fig. 9b–d) correlated with the absence of Sb-oxides, a reduction in surface Sb, and the presence of a $Ga_2O_3$ interlayer, suggesting that complete removal of all surface oxides prior to dielectric deposition may not be necessary for achieving good electrical interfaces [1]. Selected samples were remeasured after ~5 months and no change was detected in device behavior.

## 4. Discussion

GaSb is known to have a highly reactive surface and can form a thick (~3–5 nm) [10,11], complex native oxide consisting of $Sb_2O_5$, $Sb_2O_3$, $Ga_2O_3$, and $Ga_2O$ [10–12,18]. Elemental Sb can also be incorporated into the film through the reactions:

$$4GaSb + 3O_2 \rightarrow 2Ga_2O_3 + 4Sb \quad (1)$$

$$2GaSb + Sb_2O_3 \rightarrow Ga_2O_3 + 4Sb \quad (2)$$

With the production of this complex layer occurring almost instantaneously at room temperature, the resulting interface exhibits a high density of trap states, which significantly hampers the integration of GaSb with high-*k* gate dielectrics.

In recent years, plasma processing has become an increasingly important practice in the semiconductor industry; however, it is a complex technique that involves a variety of particles including electrons, ions, neutrals, radicals, atoms, and highly energetic rotational and vibrational (rv) molecules [24,25]. In our reactor, the presence of the grid limits the impact of charged ions on the sample, with the primary plasma products being highly reactive neutral hydrogen species such as $H^0$, $H_2$, $H_2^{rv}$ [24]; even so, only a limited understanding of the surface reactions is known.

In the presence of a $H_2$ plasma, the complete removal of Sb-oxide from the top-most layer of the native oxide is attributed to the ready formation of volatile species following the reaction [26]:

$$Sb_2O_5 + 10H^0 \rightarrow Sb_2O_3 + 2H_2O\uparrow + 3H_2 \rightarrow 2Sb\uparrow + 3H_2O \quad (3)$$

where the elemental Sb and water desorb from the surface. It is also possible that some $SbH_3$ is formed [26]. Conversely, $Ga_2O_3$ found on the surface is reduced to a more volatile $Ga_2O$ and water through the reaction [26]:

$$Ga_2O_3 + 4H^0 \leftrightarrow Ga_2O + 2H_2O\uparrow . \quad (4)$$

At a high enough substrate temperature the resulting $Ga_2O$ would freely desorb from the surface, eventually resulting in an oxide free surface. However, when the substrate temperature is less than that of the onset of desorption (*i.e.* <400 °C) the oxygen-deficient layer eventually covers the surface and greatly decreases the rate of $Ga_2O$ formation[11,27]. In fact, a $Ga_2O_3$ rich layer is created by the reoxidation of the $Ga_2O$ due to excess oxygen in the system arising from the production of $H_2O$ in Eq. (3) and (4), desorption of water from the reactor walls, as well as migrating $O_2$ from the decomposition of Sb-oxides:

$$2Sb_2O_5 \rightarrow 2Sb_2O_3 + 2O_2 \rightarrow 4Sb\uparrow + 5O_2 \quad (5)$$

Furthermore, $Ga_2O$ is unstable in bulk and can undergo the following disproportionation reaction [27]:

$$3Ga_2O \rightarrow 4Ga + Ga_2O_3 \quad (6)$$

Additionally, as shown in Eq. (2), Sb-oxide found near the GaSb interface reacts with the underlying GaSb substrate forming $Ga_2O_3$ and elemental Sb [12,20]. The kinetics of this reaction are greatly enhanced at temperatures above 200 °C leading to increased decomposition of the Sb-oxides [11,12]. Subsequently, the elemental Sb then desorbs leaving a $Ga_2O_3$ rich surface.

Several of the reactions observed here, in particular Eq. (5), are thermally activated and not expected to progress significantly at the nominal substrate temperatures used. However, the presence of a plasma can significantly increase the local surface temperature through the energy flux that results from energetic particle bombardment, chemical surface reactions and heat radiation. Local temperature increases of >50 °C have been reported for systems comparable to that used here [25], allowing decomposition and desorption reactions to occur at lower-than-expected nominal substrate temperatures.

Many trends observed with varying plasma power, substrate temperature, and time may, at least in part, be attributed to plasma-induced variations in local surface temperature [25]. Increasing plasma power leads to an increase in the kinetic energy of the plasma species, especially the roto-vibrationally excited hydrogen molecules ($H_2^{rv}$), which in turn increases the surface temperature [24,25]. For the powers investigated here, the surface temperature was too low for $Ga_2O$ desorption to offset the thermal transfer of oxygen, and instead of complete oxide removal, a more stable $Ga_2O_3$ layer was formed as indicated by the XPS spectra in Fig. 4.

Similarly, an increase in the substrate temperature contributes to an increased surface temperature, inducing $Ga_2O_3$ formation for substrate temperatures up to 250 °C. Conversely, at 300 °C it is conceivable that the surface temperature becomes high enough to increase the $Ga_2O$ desorption from the surface, inhibiting further $Ga_2O_3$ formation. However, the increased surface temperature also led to the decomposition of the underlying GaSb substrate, as evident from the AFM scan in Fig. 5d, where Sb from within the substrate migrated to the surface and eventually desorbed.

The trends observed with time may also be attributed to plasma-induced surface heating. Initially, when a surface is exposed to plasma, energy is transferred and the energy flux from the plasma species will exceed the heat output of the surface, causing the surface temperature to rise until a thermal equilibrium state is reached [25]. The steady state temperature is determined by a balance of energy gain from the plasma and energy loss by either conduction or radiation [25]. The time it takes to reach equilibrium varies from system to system and is dependent upon reactor design, pressure regimes, and the process gases used. Kersten et al. reported that temperature equilibrium took more than 10 min for a similar system as used in this work [25]. Therefore, it is reasonable to believe that the stark difference of the Ga 3d XPS spectra found in Fig. 8 between the (b) 10 min and (c) 20 min cases is due to the ramping up of the surface temperature. However, once the steady-state surface temperature is reached, the $Ga_2O$ desorption rate and the $Ga_2O_3$ formation rate are in equilibrium, thus minimal changes in surface chemistry are expected with additional plasma exposure time.

## 5. Conclusion

We investigated the use of an *in situ* $H_2$ plasma pre-treatment as a means to obtain a high quality electrical interface between *p*-GaSb substrates and high-*k* $Al_2O_3$ films deposited *via* PEALD. $H_2$ plasma exposure was observed to completely remove Sb-oxides, reduce elemental Sb, and increase $Ga_2O_3$ for adequate plasma parameters. Results indicate that the reaction rate for oxide removal and redistribution is a function of the density of hydrogen species, the

kinetic energy, and importantly the surface temperature, which can be adjusted by tuning the plasma power, plasma exposure time, and/or the external substrate temperature. From electrical measurements, samples exhibiting the highest capacitance modulation correlated with the highest $Ga_2O_3$ interfacial content leading to the conclusion that an oxide free surface may not be necessary for optimal electrical performance. The use of an *in situ* hydrogen plasma pre-treatment eliminates the need for wet chemical etches and may also be relevant to the deposition of alternative high-*k* dielectrics such as $HfO_2$, making it a promising technique for realizing high performance Sb-based MOS-devices.

## Acknowledgements

This work was supported by the Office of Naval Research. The authors thank James Champlain and Vic Bermudez for valuable insight and discussion, James Culbertson for AFM and Brad Pate for XPS training and guidance.

## References

[1] L.B. Ruppalt, E.R. Cleveland, J.G. Champlain, S.M. Prokes, J.B. Boos, D. Park, B.R. Bennett, Atomic layer deposition of $Al_2O_3$ on GaSb using in situ hydrogen plasma exposure, Applied Physics Letters 101 (2012).
[2] B.R. Bennett, R. Magno, J.B. Boos, W. Kruppa, M.G. Ancona, Antimonide-based compound semiconductors for electronic devices: a review, Solid-State Electronics 49 (2005) 1875–1895.
[3] R. Chau, S. Datta, M. Doczy, B. Doyle, J. Jin, J. Kavalieros, A. Majumdar, M. Metz, M. Radosavljevic, Benchmarking nanotechnology for high-performance and low-power logic transistor applications, IEEE Transactions on Nanotechnology 4 (2005) 153–158.
[4] J.A. del Alamo, Nanometre-scale electronics with III–V compound semiconductors, Nature 479 (2011) 317–323.
[5] C. Wang, M. Xu, J. Gu, D.W. Zhang, P.D. Ye, Gasb metal-oxide-semiconductor capacitors with atomic-layer-deposited HfAlO as gate dielectric, Electrochemical and Solid State Letters 15 (2012) H51–H54.
[6] A. Nainani, T. Irisawa, Z. Yuan, B.R. Bennett, J.B. Boos, Y. Nishi, K.C. Saraswat, Optimization of the $Al_2O_3$/GaSb interface and a high-mobility gasb pmosfet, IEEE Transactions on Electron Devices 58 (2011) 3407–3415.
[7] A. Ali, H. Madan, R. Misra, A. Agrawal, P. Schiffer, J.B. Boos, B.R. Bennett, S. Datta, Experimental determination of quantum and centroid capacitance in arsenide–antimonide quantum-well MOSFETS incorporating nonparabolicity effect, IEEE Transactions on Electron Devices 58 (2011) 1397–1403.
[8] E.R. Cleveland, L. Henn-Lecordier, G.W. Rubloff, Role of surface intermediates in enhanced, uniform growth rates of $TiO_2$ atomic layer deposition thin films using titanium tetraisopropoxide and ozone, Journal of Vacuum Science & Technology A 30 (2012), 01A150-1–01A150-6.
[9] E.R. Cleveland, P. Banerjee, I. Perez, S.B. Lee, G.W. Rubloff, Profile evolution for conformal atomic layer deposition over nanotopography, ACS Nano 4 (2010) 4637–4644.
[10] Z.Y. Liu, B. Hawkins, T.F. Kuech, Chemical and structural characterization of GaSb(1 0 0) surfaces treated by HCl-based solutions and annealed in vacuum, Journal of Vacuum Science & Technology B 21 (2003) 71–77.
[11] K. Moller, L. Toben, Z. Kollonitsch, C. Giesen, M. Heuken, F. Willig, T. Hannappel, In-situ monitoring and analysis of gaSb(1 0 0) substrate deoxidation, Applied Surface Science 242 (2005) 392–398.
[12] A. Ali, H.S. Madan, A.P. Kirk, D.A. Zhao, D.A. Mourey, M.K. Hudait, R.M. Wallace, T.N. Jackson, B.R. Bennett, J.B. Boos, S. Datta, Fermi level unpinning of GaSb (1 0 0) using plasma enhanced atomic layer deposition of $Al_2O_3$, Applied Physics Letters 97 (2010) 143502-1–143502-3.
[13] K. Banerjee, S. Ghosh, E. Plis, S. Krishna, Study of short- and long-term effectiveness of ammonium sulfide as surface passivation for InAs/GaSb superlattices using X-ray photoelectron spectroscopy, Journal of Electronic Materials 39 (2010) 2210–2214.
[14] T.D. Veal, M.J. Lowe, C.F. McConville, HREELS and photoemission study of GaSb(1 0 0)-(1 × 3) surfaces prepared by optimal atomic hydrogen cleaning, Surface Science 499 (2002) 251–260.
[15] A. Nainani, Y. Sun, T. Irisawa, Z. Yuan, M. Kobayashi, P. Pianetta, B.R. Bennett, J.B. Boos, K.C. Saraswat, Device quality sb-based compound semiconductor surface: a comparative study of chemical cleaning, Journal of Applied Physics 109 (2011) 114908-1–114908-7.
[16] S. McDonnell, D.M. Zhernokletov, A.P. Kirk, J. Kim, R.M. Wallace, In situ X-ray photoelectron spectroscopy characterization of $Al_2O_3$/GaSb interface evolution, Applied Surface Science 257 (2011) 8747–8751.
[17] H.-D. Trinh, E.Y. Chang, Y.-Y. Wong, C.-C. Yu, C.-Y. Chang, Y.-C. Lin, H.-Q. Nguyen, B.-T. Tran, Effects of wet chemical and trimethyl aluminum treatments on the interface properties in atomic layer deposition of $Al_2O_3$ on InAs, Japanese Journal of Applied Physics 49 (2010) 111201-1–111201-4.
[18] R.B. Konda, R. Mundle, O. Bamiduro, H. Dondapati, M. Bahoura, A.K. Pradhan, C. Donley, Effect of pulsed deposition of $Al_2O_3$ for native oxides reduction of GaAs by atomic layer deposition technique, Journal of Vacuum Science & Technology A 30 (2012), 01A118-1–01A118-4.
[19] A.D. Carter, W.J. Mitchell, B.J. Thibeault, J.J.M. Law, M.J.W. Rodwell, Al(2)O3 growth on (1 0 0) In0.53Ga0.47As initiated by cyclic trimethylaluminum and hydrogen plasma exposures, Applied Physics Express 4 (2011) 091102-1–091102-3.
[20] Z. Lu, Y. Jiang, W.I. Wang, M.C. Teich, R.M. Osgood, GaSb-oxide removal and surface passivation using an electron–cyclotron resonance hydrogen source, Journal of Vacuum Science & Technology B 10 (1992) 1856–1861.
[21] S.W. Robey, K. Sinniah, Initial etching of GaAs (0 0 1) during H-2 plasma cleaning, Journal of Applied Physics 88 (2000) 2994–2998.
[22] G.R. Bell, N.S. Kaijaks, R.J. Dixon, C.F. McConville, Atomic hydrogen cleaning of polar III–V semiconductor surfaces, Surface Science 401 (1998) 125–137.
[23] J.W. Elzey, P.F.A. Meharg, E.A. Ogryzlo, Kinetic-study of atomic-hydrogen etching of GaAs(1 0 0), Journal of Applied Physics 77 (1995) 2155–2159.
[24] P. Vankan, D.C. Schram, R. Engeln, Atomic and molecular hydrogen densities in a plasma expansion, Plasma Sources Science & Technology 14 (2005) 744–750.
[25] H. Kersten, H. Deutsch, H. Steffen, G.M.W. Kroesen, R. Hippler, The energy balance at substrate surfaces during plasma processing, Vacuum 63 (2001) 385–431.
[26] E. Weiss, O. Klin, S. Grossman, S. Greenberg, P.C. Klipstein, R. Akhvlediani, R. Tessler, R. Edrei, A. Hoffman, Hydrogen and thermal deoxidations of InSb and GaSb substrates for molecular beam epitaxial growth, Journal of Vacuum Science & Technology A 25 (2007) 736–745.
[27] M. Yamada, Y. Ide, K. Tone, Interaction of atomic-hydrogen with GaAs(0 0 1) surface oxide – volatile Ga-oxide formation, Applied Surface Science 70–71 (1993) 531–535.